Electric field induced gap modification in ultrathin blue phosphorus

Barun Ghosh,[1] Suhas Nahas,[2] Somnath Bhowmick,[2,*] and Amit Agarwal[1,†]

[1]*Department of Physics, Indian Institute of Technology Kanpur, Kanpur 208016, India*
[2]*Department of Material Science and Engineering, Indian Institute of Technology Kanpur, Kanpur 208016, India*

We investigate the possibility of band structure engineering in the recently predicted 2D layered form of blue phosphorus via an electric field (E_z) applied perpendicular to the layer(s). Using density functional theory, we study the effect of a transverse electric field in monolayer as well as three differently stacked bilayer structures of blue phosphorus. We find that for $E_z > 0.2$ V/Å the direct energy gap at the Γ point, which is much larger than the default indirect band gap of mono- and bilayer blue phosphorus, decreases linearly with the increasing electric field, becomes comparable to the default indirect band gap at $E_z \approx 0.45(0.35)$ V/Å for monolayer (bilayers), and decreases further until the semiconductor to metal transition of 2D blue phosphorus takes place at $E_z \approx 0.7(0.5)$ V/Å for monolayer (bilayers). Calculated values of the electron and hole effective masses along various high symmetry directions in the reciprocal lattice suggests that the mobility of charge carriers is also influenced by the applied electric field.

I. INTRODUCTION

Various 2D crystals such as graphene [1–4], silicene [5–9], germanene [6,10,11], transition metal dichalcogenides (MoS_2, $MoSe_2$, WSe_2, etc.) [12–14] are being actively explored for the post Si nanoelectronics era, for their promise of aggressive channel length scalability on account of reduced short channel effects [15]. Field effect transistors (FET's) based on graphene [16], and MoS_2 [17], have already been demonstrated with performance which is superior to conventional Si based FET's. Layered black phosphorus (dubbed phosphorene) has joined this exciting family of 2D crystals of late, and FET's based on few layer black phosphorus have been fabricated with I_{ON}/I_{OFF} current ratio of $\sim 10^5$, and field effect mobility of ~ 1000 cm^2/Vs [18–20].

More recently it has been predicted that, by certain dislocation of constituent P atoms, the puckered structure of black phosphorus (rectangular unit cell) can be converted to a more symmetric buckled structure (hexagonal unit cell) of another 2D allotrope, termed as the blue phosphorus [21,22]. The newly proposed allotrope is actually a single layer of the A7 phase of phosphorus [23]. Based on first principles calculations, a single layer of blue phosphorus is predicted to be as stable as monolayer black phosphorus [21,22]. Interestingly, electronic band structure of the two allotropes differ significantly. Unlike monolayer black phosphorus, which has an intrinsic direct band gap of ~ 1 eV at the Γ point, monolayer blue phosphorus has an indirect band gap of ~ 2 eV, based on GGA calculations which are well known to underestimate the band gap [21,22]. For the case of phosphorene, it has been shown that the band gap of black phosphorus depends on the number of layers [19], strain [24], and applied electric field (perpendicular to the layers) [25]. Such electronic band structure engineering in various 2D materials is essential for increasing their usefulness for application in various nanoelectronic and nanophotonic devices.

In this paper we focus on electric field induced band-gap modification in mono- and bilayer blue phosphorus. Such materials with tunable band gap, particularly by means of a transverse electric field, would allow for flexibility and optimization of their usage in various devices. For example, in FET's the gate voltage is applied perpendicular to the plane of the 2D material, which necessitate detailed understanding of the effect of transverse electric field on its electronic band structure. The effect of transverse electric field on the electronic properties has earlier been studied both theoretically and experimentally for various 2D materials such as graphene [26,27], silicene [28,29], germanene [29], transition metal dichalcogenides such as MoS_2 [30,31], black phosphorus [25], etc.

For this paper we use *ab initio* density functional theory calculations to study the electric field induced gap modification in mono- and bilayer blue phosphorus with three different stackings [see Figs. 1(a)–1(d)]. All four (one monolayer and three bilayer) crystals, have an intrinsic indirect band gap. With increasing electric field, the direct band gap at the Γ point decreases almost linearly and becomes comparable to other indirect band gaps, which on further increase of the electric field vanishes, leading to an insulator-metal transition. The paper is organized in the following sequence: We describe the parameters used for DFT calculation and the crystal structure of monolayer and differently stacked bilayer blue phosphorus in Sec. II. This is followed by a detailed discussion of the dependence of the band gap and the electron and hole effective mass on the strength of transverse electric field in Sec. III. Finally we summarize our results in Sec. IV.

II. CRYSTAL STRUCTURE OF MONOLAYER AND BILAYER BLUE PHOSPHORUS

The *ab initio* calculations are performed by density functional theory (DFT), using a plane-wave basis set and norm-conserving Troullier Martins pseudopotential, as implemented in Quantum Espresso [32]. Electron exchange and correlation is treated within the framework of generalized gradient approximation (GGA-PBE) [33] and a hybrid functional, HSE06 [34].
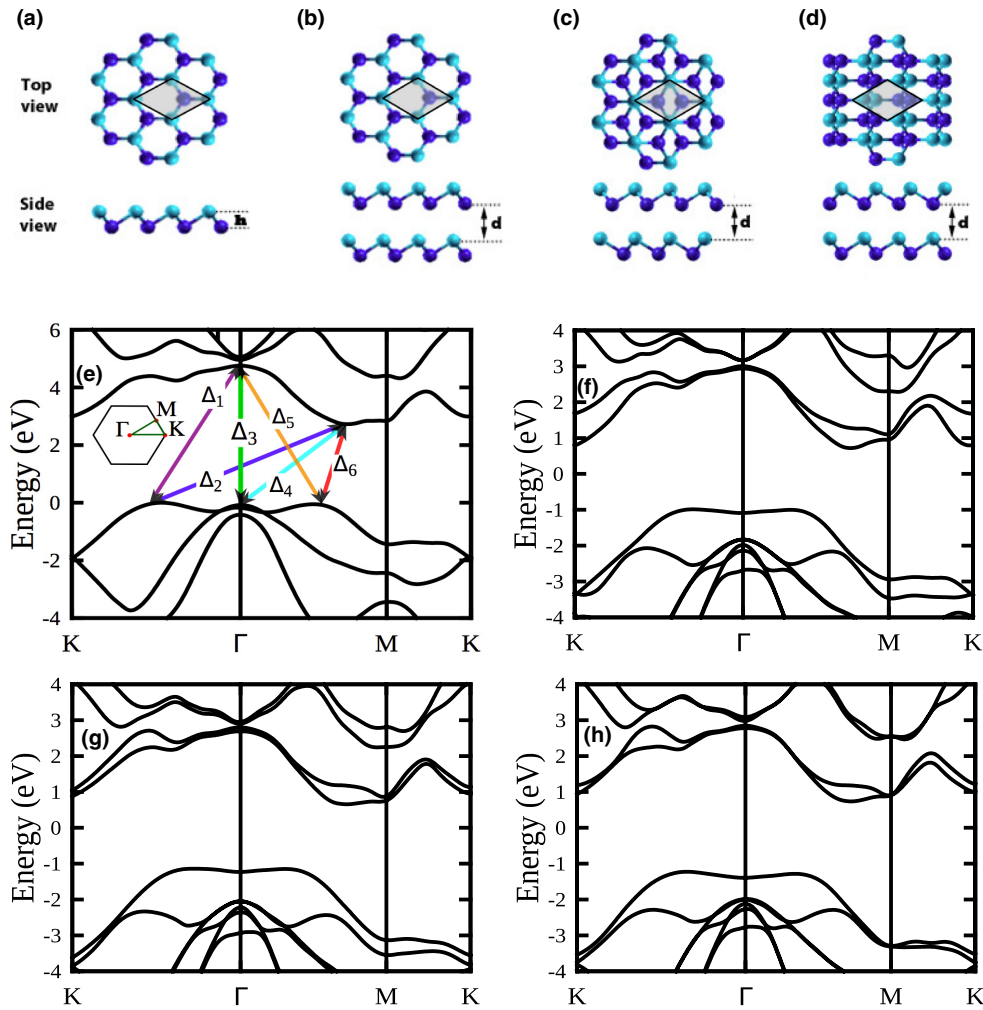
----

*bsomnath@iitk.ac.in
†amitag@iitk.ac.in

FIG. 1. (Color online) Panels (a), (b), (c), and (d) display the layered structure and panels (e), (f), (g), and (h) show the electronic band structure of monolayer, AA, AB, and AC stacked bilayer blue phosphorus, respectively. Atoms located at the top and bottom of the quasiplanar layers are distinguished by cyan and dark blue color, respectively, and they form two interpenetrating hexagonal sublattices. The shaded area in (a)–(d) represents the unit cell. Panel (e) defines different energy gaps between valence and conduction band, whose electric field dependence is illustrated in Fig. 3. The intrinsic indirect band gap is equal to $\triangle_2$ in all four structures.

All the structures were optimized using the PBE functional coupled to DFT-D2 method as prescribed in Ref. [35] to incorporate van der Waal's correction. Similar methods to relax black phosphorus have been shown to produce results that closely match experimental data [36], thereby justifying our approach. As a validation of our HSE06 calculations, we have reproduced the band structure of black phosphorene given in Ref. [36]. Since the trend and qualitative nature of all the results obtained using GGA and HSE06 are similar, and HSE06 has been demonstrated to give a better estimation of the electronic properties of black phosphorene [36], only the HSE06 based results are shown, unless stated otherwise. The kinetic energy cutoff for wave function is set to be 120 Ry. A supercell with a vacuum of 25 Å along the z direction (perpendicular to the blue phosphorus layers) is constructed to eliminate the interaction with spurious replica images. A k-point grid of $12 \times 12 \times 1$ is used for the Brillouin zone integrations. Structural relaxations are carried out until the force on each atom (total energy change due to ionic relaxation between two successive steps) is less than 10^{-5} Ry/au (10^{-6} Ry). An external sawtooth potential

is used in the z direction to simulate the effect of an applied electric field perpendicular to the blue phosphorus layer(s).

We now describe the crystal structure of mono- and bilayer blue phosphorus. The honeycomb net of P atoms in monolayer blue phosphorus is formed by two interpenetrating hexagonal sublattices [shown in two different colors/shades in Fig. 1(a)]. However, unlike graphene and similar to silicene/germanene, the two sublattices in blue phosphorus are not in the same plane and the vertical distance between them is given by h [as shown Fig. 1(a), $h = 1.24$ Å]. This results in a pseudoplanar structure, where half of the atoms are buckled out of the plane, with a P-P bond angle equal to $92.9°$. Each of these monolayers can be stacked so as to form multilayered structures in different ways, based on the relative displacement of the sublattices of one layer with respect to the other layers. In this paper, we consider bilayers stacked in three different sequences, namely AA [Fig. 1(b)], AB [Fig. 1(c)], and AC [Fig. 1(d)]. The unit cell has four atoms in total, two each in every layer. In case of AA stacking, the two sublattices belonging to each of the layers overlap directly, and as a consequence, only two atoms per unit

TABLE I. Equilibrium structural parameters for monolayer and differently stacked bilayer blue phosphorus.

Stacking	Bond length (Å)	Bond angle (Degree)	d (Å)
Mono	2.27	92.88	
AA	2.26	93.06	3.23
AB	2.26	93.13	3.20
AC	2.27	93.00	3.41

cell are visible in the top view [see Fig. 1(b)]. On the contrary, one constituent layer is displaced relative to the other one by a P-P bond length in case of AB stacking, such that one of the two sublattices of both the layers overlap directly and the other sublattice of the first layer is placed on top of the center of the honeycomb net of the second layer. Consequently, only three atoms per unit cell are visible in the top view of AB-stacked bilayer blue phosphorus, as shown in Fig. 1(c). Similar to AB, one layer of blue phosphorus is displaced with respect to the other one in case of AC stacking as well. However, unlike AB, none of the sublattices from the two layers are located directly on top of each other and thus, as illustrated in Fig. 1(d), all four atoms per unit cell are visible in the top view. As reported in Table I, although the bond length and bond angle are nearly equal, irrespective of stacking sequence, the interplanar spacing d changes significantly; for example AC (maximum d) has 6% more interplanar spacing than AB (minimum d). Similarly, total energy of bilayer blue phosphorus also depends on the stacking sequence, AA being energetically the most favorable one, followed by AC and AB, having 0.1 meV/atom and 2 meV/atom higher energy than AA.

Electronic band structure is calculated along various high symmetry directions in the reciprocal lattice [see the inset of Fig. 1(e)] and the energy dispersion relations are shown in Fig. 1(e)–1(h). As illustrated in the figure, we define six different values of energy gap between the valence and conduction band, namely $\triangle_1$, $\triangle_2$, $\triangle_3$, $\triangle_4$, $\triangle_5$, and $\triangle_6$, and among them $\triangle_3$ is the only direct energy gap (measured at the Γ point). The choice is made on the basis of the fact that the actual band gap of mono- or bilayer blue phosphorus in zero or finite electric field is equal to one of the $\triangle_i$'s, as defined in Fig. 1(e). For example, in zero electric field single layer of blue phosphorus is an indirect band gap semiconductor and the band gap is equal to $\triangle_2$ [see Fig. 1(e)]. The electronic band structure is qualitatively similar for both GGA and HSE06 based calculations, although the magnitude of the band gap differs significantly: 1.94 eV (GGA) and 2.73 eV (HSE06), respectively, and the values for GGA compare well with those reported in the literature [21]. Similarly, bilayer blue phosphorus is also an indirect band-gap semiconductor, and the band gap is equal to $\triangle_2$ for all three stacking sequences (AA, AB, and AC) although $\triangle_6 \sim \triangle_2 \sim \triangle_4$ [see Figs. 1(f)–1(h)]. Depending on the stacking sequence, the magnitude of the band gap of bilayer blue phosphorus is 1.0 eV (GGA)–1.74 eV (HSE06) for AA, 0.97 eV (GGA)–1.80 eV (HSE06) for AB, and 1.14 eV (GGA)–1.97 eV (HSE06) for AC, almost 40–50% less than that of monolayer blue phosphorus for all three bilayer structures.

III. BAND GAP AND EFFECTIVE MASS DEPENDENCE ON THE TRANSVERSE ELECTRIC FIELD

We now explore the effect of an externally applied transverse electric field on the electronic band structure of monolayer and bilayer blue phosphorus. For this purpose, an electric field is applied in a direction perpendicular to the blue phosphorus layer (ranging from 0.1 V/Å to 0.7 V/Å, in steps of 0.1 V/Å), which is similar to applying a gate voltage in FET's. We find that, unlike silicene [29], electric field does not affect the buckling in the case of blue phosphorus (value of h changes by 0.28% when the strength of electric field is increased from 0 to 0.7 V/Å) and other structural parameters like bond length and bond angle also do not change significantly. Although there is no considerable structural modification, electronic band structure changes substantially, particularly at higher values of applied electric field [see Figs. 2(a) and 3(a)]. As shown in the figure, up to 0.2 V/Å the electronic band structure of monolayer blue phosphorus is mostly unaffected by the applied field and the change is readily apparent only when the applied field is 0.3 V/Å or more. Interestingly, the most significant change occurs at the conduction band edge at the Γ point, which starts shifting towards the VBM, and as a result the value of $\triangle_1$, $\triangle_3$, and $\triangle_5$ decreases with increasing electric field, while $\triangle_2$, $\triangle_4$, and $\triangle_6$ do not change appreciably [see Fig. 3(a)]. As illustrated in Fig. 3(a), monolayer blue phosphorus remains an indirect band-gap (magnitude equal to $\triangle_2$) semiconductor up to 0.45 V/Å applied field. However, when the electric field is increased further to 0.5 V/Å the downward shift of conduction band edge at the Γ point is so large that the conduction band minima (CBM) is relocated to the Γ point (from its original position, in the middle of Γ-M), converting monolayer blue phosphorus to a semiconductor with comparable direct and indirect band gaps ($\triangle_3 \sim \triangle_1 \sim \triangle_5$) [see Figs. 2(a) and 3(a)]. Note that the valence band maxima does not change significantly even at higher electric field; although it shifts to close the band gap at 0.7 V/Å applied field, valence band maxima (VBM) retains its location in the middle of the K-Γ direction.

Similar to the monolayer, structural parameters of bilayer blue phosphorus, like bond length, bond angle, and buckling (h), are hardly affected by externally applied electric field and interplanar spacing changes, only by 3.22% in AA, 4.5% in AB, and 2.35% in AC, as the electric field increases from 0 to 0.5 V/Å. Like a single layer of blue phosphorus, the most significant change to the electronic band structure also occurs at the conduction band edge at the Γ point, which gradually shifts downward with increasing electric field, starting from 0.3 V/Å and higher [see Figs. 2(b)–2(d)]. As a result, the conduction band minima, which is originally located approximately in the middle of Γ-M, is shifted to the Γ point at 0.35 V/Å electric field [see Figs. 2(b)–2(d)]. Consequently, the band gap changes from $\triangle_2$ to $\triangle_1$ (which is also comparable to $\triangle_3$ and $\triangle_5$) in all three structures [see Figs. 3(b)–3(d)].

Having discussed the effect of transverse electric field on the band gap, we move on to the effective mass which determines the electron/hole mobility and thus also controls the transport properties. From the energy dispersion relation, the effective mass is calculated both at VBM (m_h^*) and CBM (m_e^*). As shown in Fig. 4(a), the effective mass of holes (m_h^*) does not change
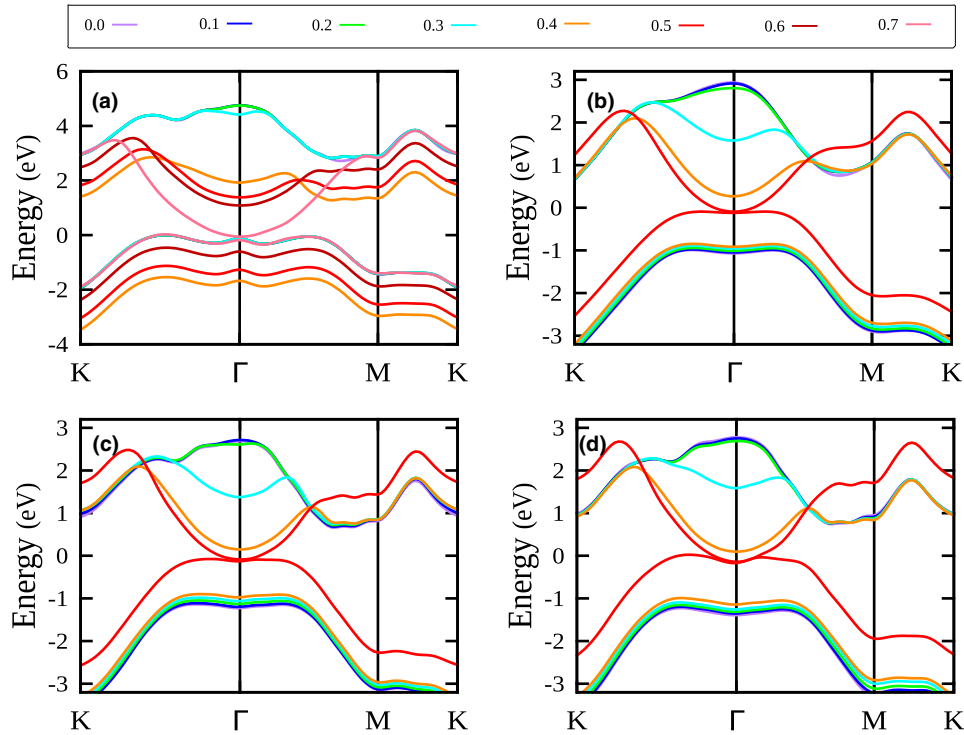
FIG. 2. (Color online) Panels (a), (b), (c), and (d) study the effect of the transverse electric field on the lowest conduction band and highest valance band for monolayer, AA, AB, and AC stacked bilayer blue phosphorus, respectively. Note that for all four cases, the direct band gap at the Γ point [$\triangle_3$, as defined in Fig. 1(e)] decreases with increasing electric field, while the default indirect band gap almost remains constant. The transition from wide-gap indirect semiconductor to a narrow-gap direct semiconductor and eventually to a metal with increasing electric field is evident in all four plots.
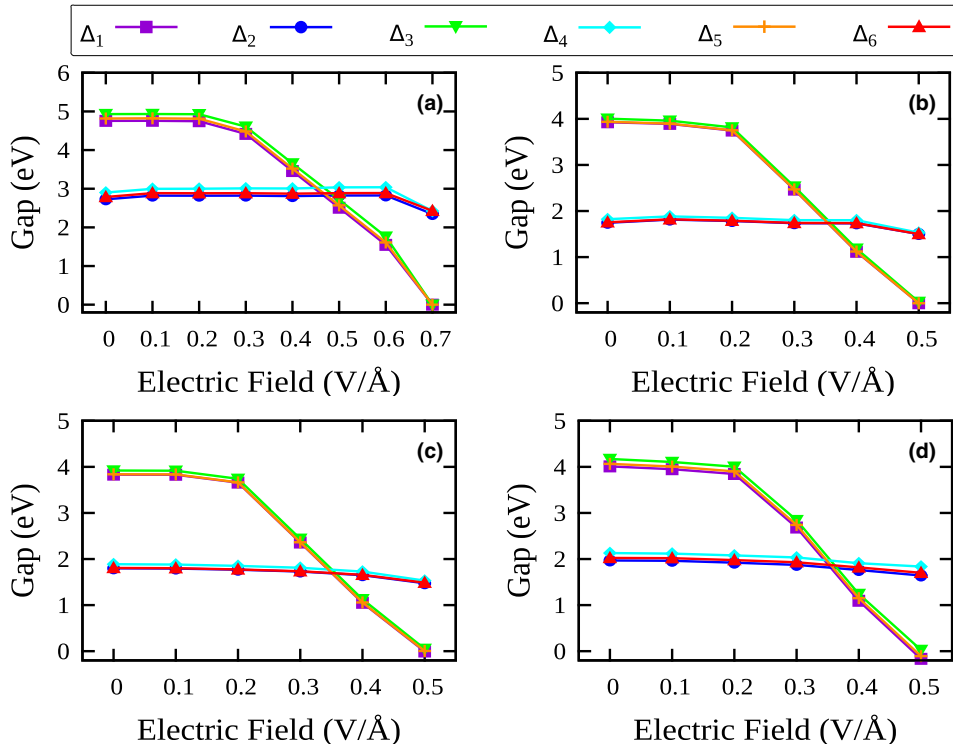

FIG. 3. (Color online) Panels (a), (b), (c), and (d) study the effect of the transverse electric field on the various band gaps specified in Fig. 1(e), for monolayer, AA, AB, and AC stacked bilayer blue phosphorus, respectively. Note that Δ_3 (green triangle pointing downwards) denotes the direct band gap at the Γ point, while all other Δ's represent indirect band gaps. In all the panels, the direct band gap at the Γ point decreases with increasing electric field, and becomes comparable to the indirect band gap, and both of which vanish for electric field strength of $\sim$0.7(0.5) V/Å making monolayer (bilayer) blue phosphorus metallic.
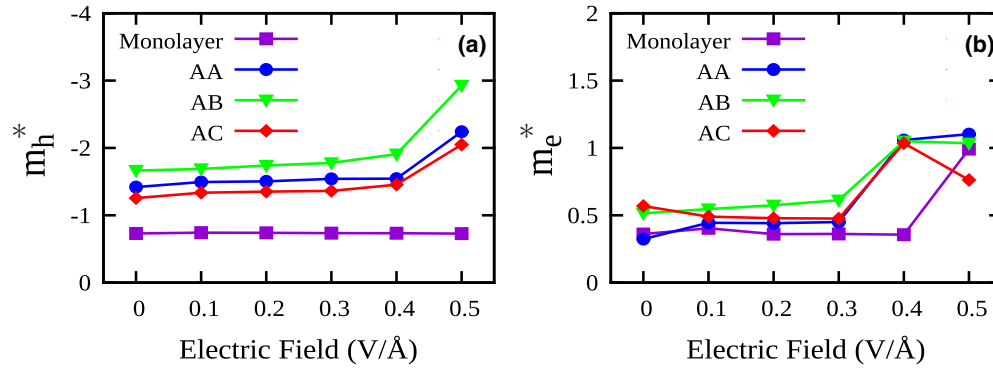
FIG. 4. (Color online) Panels (a) and (b) display the variation of hole and electron effective mass at valence band maxima (VBM) and conduction band minima (CBM) for monolayer and differently stacked bilayer blue phosphorus. If the VBM or CBM occurs in the middle of ΓM or ΓK, the effective mass is calculated in that particular direction. Otherwise, at the Γ point, it is found to be isotropic.

significantly as a function of the transverse electric field, since the shape of the valence bands is not affected by the transverse electric field [see Fig. 2]. However, depending on the number of layers and stacking sequence m_e^* increases by a factor of 1.5 to 4 with increasing electric field [see Fig. 4(b)], which can be attributed to the shifting of CBM to the Γ point from its original location at zero or smaller electric field.

IV. CONCLUSION

To summarize, we have explicitly shown that monolayer and bilayers of blue phosphorus are versatile 2D materials in which the band gap can be tuned from ∼2.73 eV (HSE06) [∼1.74 eV (HSE06)] for monolayer (bilayer) to 0 eV, by means of a transverse electric field. Broadly, we find that the intrinsic indirect band gap remains constant while the direct band gap

at the Γ point, and another two indirect band gaps, decrease (almost linearly) with increasing electric field. Both monolayer and bilayer blue phosphorus undergo a transition from indirect band gap insulator to a direct band gap insulator for $E_z \geqslant$ 0.45(0.35) V/Å for monolayer (bilayers), and eventually to metal for $E_z \geqslant 0.7(0.5)$ V/Å for monolayer (bilayers). All these changes in the band structure are also reflected in the effective mass.

[1] A. K. Geim and K. S. Novoselov, The rise of graphene, Nat. Mater. **6**, 183 (2007).

[2] A. H. Castro Neto, F. Guinea, N. M. R. Peres, K. S. Novoselov, and A. K. Geim, The electronic properties of graphene, Rev. Mod. Phys. **81**, 109 (2009).

[3] M. I. Katsnelson, *Graphene* (Cambridge University Press, Cambridge, 2012).

[4] E. J. G. Santos and E. Kaxiras, Electricfield dependence of the effective dielectric constant in graphene, Nano Lett. **13**, 898 (2013).

[5] K. Takeda and K. Shiraishi, Theoretical possibility of stage corrugation in Si and Ge analogs of graphite, Phys. Rev. B **50**, 14916 (1994).

[6] G. G. Guzmán-Verri and L. C. Lew Yan Voon, Electronic structure of silicon-based nanostructures, Phys. Rev. B **76**, 075131 (2007).

[7] B. Lalmi, H. Oughaddou, H. Enriquez, A. Kara, S. Vizzini, B. Ealet, and B. Aufray, Epitaxial growth of a silicene sheet, Appl. Phys. Lett. **97**, 223109 (2010).

[8] P. Vogt, P. De Padova, C. Quaresima, J. Avila, E. Frantzeskakis, M. C. Asensio, A. Resta, B. Ealet, and G. Le Lay, Silicene: Compelling experimental evidence for graphene like two-dimensional silicon, Phys. Rev. Lett. **108**, 155501 (2012).

[9] L. Chen, C.-C. Liu, B. Feng, X. He, P. Cheng, Z. Ding, S. Meng, Y. Yao, and K. Wu, Evidence for dirac fermions in a honeycomb lattice based on silicon, Phys. Rev. Lett. **109**, 056804 (2012).

[10] E. Bianco, S. Butler, S. Jiang, O. D. Restrepo, W. Windl, and J. E. Goldberger, Stability and exfoliation of germanane: A germanium graphane analogue, ACS Nano **7**, 4414 (2013).

[11] S. Cahangirov, M. Topsakal, E. Aktürk, H. Şahin, and S. Ciraci, Two- and one-dimensional honeycomb structures of silicon and germanium, Phys. Rev. Lett. **102**, 236804 (2009).

[12] M. Chhowalla, H. S. Shin, G. Eda, L.-J. Li, K. P. Loh, and H. Zhang, The chemistry of two-dimensional layered transition metal dichalcogenide nanosheets, Nat. Chem. **5**, 263 (2013).

[13] X. Xu, W. Yao, D. Xiao, and T. F. Heinz, Spin and pseudospins in layered transition metal dichalcogenides, Nat. Phys. **10**, 343 (2014).

[14] E. J. G. Santos and E. Kaxiras, Electrically driven tuning of the dielectric constant in MoS$_2$ layers, ACS Nano **7**, 10741 (2013).

[15] G. Fiori, F. Bonaccorso, G. Iannaccone, T. Palacios, D. Neumaier, A. Seabaugh, S. K. Banerjee, and L. Colombo, Electronics based on two-dimensional materials, Nat. Nanotechnol. **9**, 768 (2014).

[16] F. Schwierz, Graphene transistors, Nat. Nanotechnol. **5**, 487 (2010).

[17] B. Radisavljevic, A. Radenovic, J. Brivio, V. Giacometti, and A. Kis, Single-layer MoS$_2$ transistors, Nat. Nanotechnol. **6**, 147 (2011).

[18] L. Li, Y. Yu, G. J. Ye, Q. Ge, X. Ou, H. Wu, D. Feng, X. H. Chen, and Y. Zhang, Black phosphorus field-effect transistors, Nat. Nanotechnol. **9**, 372 (2014).

[19] H. Liu, A. T. Neal, Z. Zhu, Z. Luo, X. Xu, D. Tománek, and P. D. Ye, Phosphorene: An unexplored 2d semiconductor with a high hole mobility, ACS Nano **8**, 4033 (2014).

[20] S. P. Koenig, R. A. Doganov, H. Schmidt, A. H. Castro Neto, and B. Özyilmaz, Electric field effect in ultrathin black phosphorus, Appl. Phys. Lett. **104**, 103106 (2014).

[21] Z. Zhu and D. Tománek, Semiconducting layered blue phosphorus: A computational study, Phys. Rev. Lett. **112**, 176802 (2014).

[22] J. Guan, Z. Zhu, and D. Tománek, Phase coexistence and metal-insulator transition in few-layer phosphorene: A computational study, Phys. Rev. Lett. **113**, 046804 (2014).

[23] S. E. Boulfelfel, G. Seifert, Y. Grin, and S. Leoni, Squeezing lone pairs: The A17 to A7 pressure-induced phase transition in black phosphorus, Phys. Rev. B **85**, 014110 (2012).

[24] A. S. Rodin, A. Carvalho, and A. H. Castro Neto, Strain-induced gap modification in black phosphorus, Phys. Rev. Lett. **112**, 176801 (2014).

[25] J. Dai and X. C. Zeng, Bilayer phosphorene: Effect of stacking order on bandgap and its potential applications in thin-film solar cells, J. Phys. Chem. Lett. **5**, 1289 (2014).

[26] E. V. Castro, K. S. Novoselov, S. V. Morozov, N. M. R. Peres, J. M. B. L. dos Santos, J. Nilsson, F. Guinea, A. K. Geim, and A. H. Castro Neto, Biased bilayer graphene: Semiconductor with a gap tunable by the electric field effect, Phys. Rev. Lett. **99**, 216802 (2007).

[27] Y. Zhang, T.-T. Tang, C. Girit, Z. Hao, M. C. Martin, A. Zettl, M. F. Crommie, Y. R. Shen, and F. Wang, Direct observation of a widely tunable bandgap in bilayer graphene, Nature (London) **459**, 820 (2009).

[28] N. D. Drummond, V. Zólyomi, and V. I. Fal'ko, Electrically tunable band gap in silicene, Phys. Rev. B **85**, 075423 (2012).

[29] Z. Ni, Q. Liu, K. Tang, J. Zheng, J. Zhou, R. Qin, Z. Gao, D. Yu, and J. Lu, Tunable bandgap in silicene and germanene, Nano Lett. **12**, 113 (2012).

[30] Q. Liu, L. Li, Y. Li, Z. Gao, Z. Chen, and J. Lu, Tuning electronic structure of bilayer MoS$_2$ by vertical electric field: A first-principles investigation, J. Phys. Chem. C **116**, 21556 (2012).

[31] A. Ramasubramaniam, D. Naveh, and E. Towe, Tunable band gaps in bilayer transition-metal dichalcogenides, Phys. Rev. B **84**, 205325 (2011).

[32] P. Giannozzi *et al.*, Quantum espresso: a modular and open-source software project for quantum simulations of materials, J. Phys.: Condens. Matter **21**, 395502 (2009).

[33] J. P. Perdew, K. Burke, and M. Ernzerhof, Generalized gradient approximation made simple, Phys. Rev. Lett. **77**, 3865 (1996).

[34] J. Heyd, G. E. Scuseria, and M. Ernzerhof, Hybrid functionals based on a screened coulomb potential, J. Chem. Phys. **118**, 8207 (2003).

[35] S. Grimme, Semiempirical GGA-type density functional constructed with a long-range dispersion correction, J. Comput. Chem. **27**, 1787 (2006).

[36] J. Qiao, X. Kong, Z.-X. Hu, F. Yang, and W. Ji, High-mobility transport anisotropy and linear dichroism in few-layer black phosphorus, Nat. Commun. **5**, 4475 (2014).